The electronic structure study of Fe L$_3$ edge in CuFeO$_2$

O. M. ÖZKENDIR
Faculty of Technical Education, University of Mersin, Tarsus-Turkey

The electronic structure of Fe in antiferromagnetic delafossite CuFeO$_2$ were studied by using x-ray absorption fine structure (XAFS) spectroscopy around Fe L$_3$ absorption edge. The fundamental electronic and crystal structures of delafossite CuFeO$_2$ are analyzed with electronic and magnetic behavior of metal iron L and K-edge. Magnetic properties of metal Fe K-edge and L$_{2,3}$-edges are probed by X-ray Magnetic Circular Dichroism (XMCD) calculations. The calculations are based on different choices of one electron potentials by using the real space multiple scattering method FEFF 8.2 code.

1. Introduction

The ferromagnetic materials have attracted considerable attention both for their important semiconducting properties as well as for their magnetic properties because of the possibility of showing gigantic magneto-electric effects [1-3]. Iron is a ferromagnetic member of 3d transition metals which is widely used in many fields of technology. But like most of the iron oxides, delafossite CuFeO$_2$ has antiferromagnetic properties with space group R $\bar{3}$ m. Low dimensional transition metal oxides became more important since the discovery of the high temperature superconductors because of their strongly correlated electron systems [4].

Low dimensional triangular structure of CuFeO$_2$ consists of hexagonal layers. In delafossite CuFeO$_2$ structure, magnetic Fe^{+3} layers form triangular lattices which are separated by nonmagnetic Cu^{+1} and O^{-2} layers [4]. However, Oxygen nonstoichiometry largely affects the antiferromagnetism of CuFeO$_2$ single crystal by accompanying changes of cation valence band lattice parameters [5].

The electronic and magnetic properties of 3d transition metals are reflected by their *d* valence electrons [6, 7]. Core electrons are excited in the absorption process into the unoccupied states above the Fermi energy and thereby can act as a probe of the electronic and magnetic properties of the empty valence band. All the states below the Fermi level are totally filled. Since x-ray absorption spectra are governed by the dipole selection rules, the d-shell properties are best probed by L-edge absorption studies. Properties of 3d transition metals are best investigated by the x-ray absorption spectroscopy techniques by excitation of L$_{2,3}$ shell electrons to empty 3d states because of their convenient symmetries due to the atomic selection rules in the electric dipole approximation. The L$_{2,3}$-edge x-ray absorption spectra contains the details of the electronic transitions from 2p level to empty 3d and 4p levels.

K-edge transition spectra of 3d metals have characteristic white lines because of the forbidden transition from 1s to 3d shell due to atomic selection rules in the electric dipole approximation. However, L-edge absorption spectra are characterized by strong absorption resonances, called as white lines, near the L$_3$ and L$_2$ thresholds which are directly proportional to the number of d holes [8-10]. White lines in the 3d transition metals occur due to the transitions from 2p to hybridized unoccupied d states.

X-ray Absorption (XAS) spectra of 3d transition metals can offer detailed information about the atomic and magnetic orientations [11]. In order to probe the electronic structure of materials, the X-ray absorption fine structure (XAFS) spectroscopy is one of the best and mostly used techniques. XAFS provides an important method to investigate the electronic structure calculations, bondings, valency properties, catalytic properties, orbital and atomic configurations [12]**.** Near-edge XAS (XANES) spectroscopy is sensitive to inner-shell ionization process observed in x-ray absorption and also can be sensitive to interatomic distances, local coordination and local electronic structure. The shape of XANES spectrum is related to the electronic structure of the material. The oscillation observed in the high energy part of the spectrum, called as the Extended-XAFS (EXAFS) region, is associated with the arrangement of the atoms. It contains signals of interference of outgoing electron wave functions and scattered electron wave functions which carries information about the neighboring atoms, their regional configurations, atomic distances, coordination numbers etc. It is known that EXAFS amplitudes exhibit a dependence on temperature which is caused by thermal vibrations of absorbing and scattering atoms [13]. To understand the origins of various features, it is necessary to calculate the observed fine structures from a suitable theoretical model.

To probe the spin characters of the magnetic materials, one needs to use polarized x-rays in absorption studies. X-ray Magnetic Circular Dichroism (XMCD)

technique is one of the best ways to probe the magnetic properties of the ferromagnetic materials. Erskine and Stern [14] firstly suggested XMCD in investigations of magnetic properties and Schütz and coworkers [15,16] are the pioneers of the applications in the near-edge and extended fine-structure regimes. The advantages of XMCD Spectroscopy technique over the other classical techniques are; its being element-specific, chemical sensitivity, sub monolayer sensitivity and its quantitative determination of spin and orbital magnetic moments and their anisotropies [17-22]. Also, XMCD is one of the best tools which provide information on the magnetic moments of neighboring atoms of the absorber atom, besides its structural and electronic properties. It takes advantages of sensitivity in detection of very small magnetic moments.

In this paper, electronic and magnetic properties of ferromagnetic Fe foil and antiferromagnetic $CuFeO_2$ structure are investigated by using X-ray Absorption Fine structure and X-ray Magnetic Circular Dichroism spectroscopy with a particular emphasis on the numerical simulations of the K and L-edge in the absorption spectra of Fe. With this purpose full multiple scattering calculations have been performed.

2. Material and method

Fe $L_{2,3}$-edge x-ray absorption fine structure (XAFS) and X-ray magnetic circular dichroism (XMCD) calculations of delafossite $CuFeO_2$ and metal Fe foil were performed using FEFF 8.2 code, which is based on real space multiple scattering approach [23]. For the calculations, the FEFF input file was generated by the ATOMS package. The full multiple scattering calculations for 10 angstroms thick metal Fe foil thin film (containing 339 Fe atoms cluster) and 10 angstroms thick delafossite $CuFeO_2$ thin film (containing 206 atoms cluster (Fe, Cu, O)) were performed with self-consistent potential. Backscattering and phase shift with single and multiple scattering paths have been calculated to obtain the X-ray absorption spectrum. Also by XMCD, spin properties of valence electrons of Fe atoms in metal Fe foil are calculated. Calculations are performed for one Fe atom selected as an X-ray absorber and also a photoelectron emitter at 300 K temperature. Mainly, bonding effects on Fe atoms in $CuFeO_2$ structure during obtaining a delafossite $CuFeO_2$ are investigated. Electronic properties of ferromagnetic iron and antiferromagnetic delafossite $CuFeO_2$ are compared to specify the structural, electronic and magnetic changes in the transformation process from ferromagnetic to antiferromagnetic structure.

3. Results and discussion

In Fig. 1, the theoretically calculated and measured XAFS spectra of Fe L_3 and L_2 edges in metal Fe foil are shown. Metallic Fe atom has electronic configuration of [Ar] $4s^2$ $3d^6$. Empty 3d levels are located well above the Fermi level. Calculated spectra is compared with the experimental data of Ufuktepe et al taken at SSRL [24]. The theoretical calculations are consistent with the experimental results.
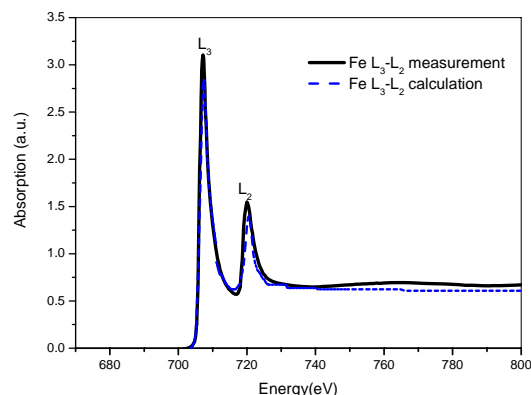
Fig. 1. Comparison of measured and calculated normalized XAFS spectra of Fe L_3 and L_2 edges for Fe foil.

The calculations are based on different choices of one electron potentials according to Fe atoms by using the real space multiple scattering method FEFF 8.2 code [13, 25]. The Fe metal L-edge spectra mainly show two broad peaks which are related with the width of the empty d-bands. First maximum at 707 eV corresponds to the transition from $2p_{3/2}$ electrons at L_3-edge to 3d state. Second maximum at 720 eV corresponds to the transition from $2p_{1/2}$ electrons at L_2-edge to 3d state. Strong $L_{2,3}$ peaks are called as white lines which are related to directly with the hole potentials at valence 3d state.

In Fig. 2, calculated L_3 and L_2-edge XMCD spectra of ferromagnetic metal Fe foil are given within the inset of Fe $L_{2,3}$ XAFS spectra. The XMCD probes the spin properties of empty valance states in magnetic materials. In such magnetic materials, the empty states cause imbalanced magnetic moments. However, if an electron excites to a final state which is forbidden due to electric dipole approximation, strong spin orbit coupling can occur as a result of mixing between 3d-4p final states. According to electric dipole transitions, electrons of any core level with right polarized "spin-up" or left-polarized "spin-down" character can be excited into a final state with convenient spin symmetry. In figure 2, L_3 ($2p_{3/2}$) electrons excites to an empty 3d "spin-down" state, however L_2 ($2p_{1/2}$) electrons transits to high energy "spin-up" level of mixed 3d-4p state. According to calculated XMCD spectra, the magnetic moment of the Fe metal is calculated as 2.27 μ_B /atom by the sum rules.
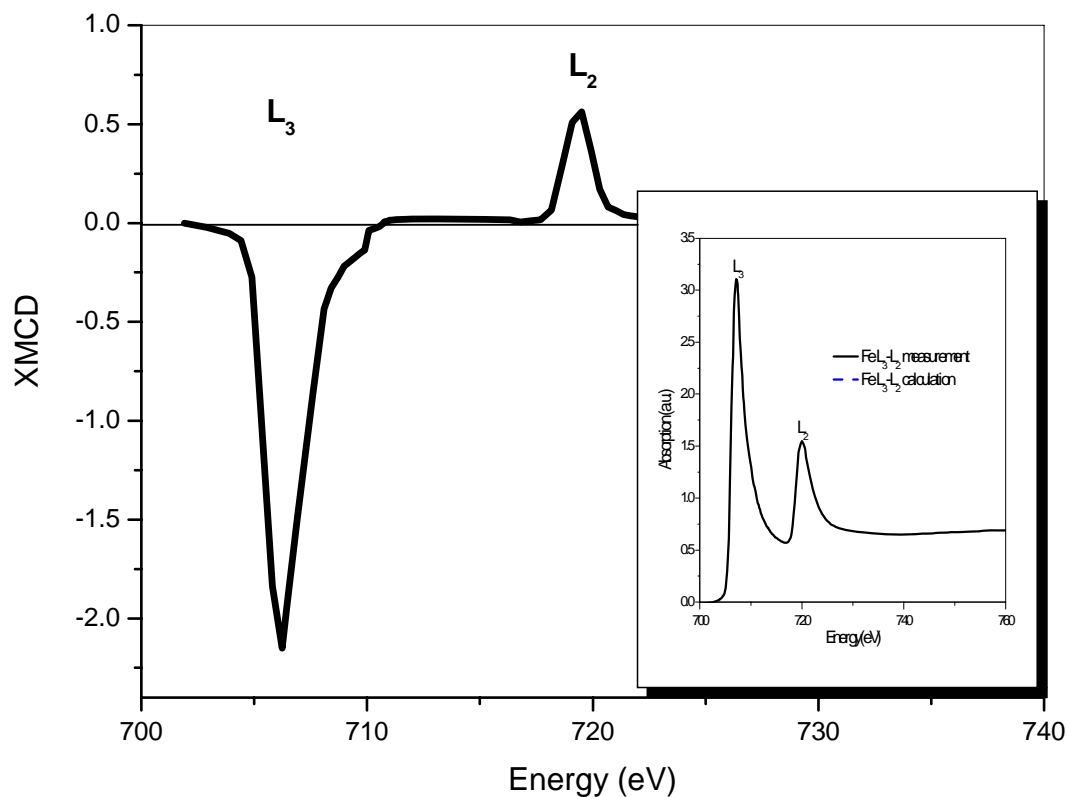
Fig. 2. Calculated L_3 and L_2-edge XMCD spectra of ferromagnetic metal Fe foil are given within the inset of Fe $L_{2,3}$ XANES spectra.

Comparison of XAFS and XMCD calculation of Fe K-edge absorption spectra for Fe foil is given in Fig. 3. Fe K-edge absorption spectrum begin to rise at 7111 eV energy. Spectrum has a shoulder like pre-edge peak "A" which corresponds to forbidden transition by the atomic selection rules in the electric dipole approximation from 1s core level to t_{2g} low levels of 3d at 7115 eV. Pre-edge A is observed in XMCD spectrum of Fe K-edge, as a 1s spin-up electron transition to an empty spin-up state in 3d. Beyond this peak, K-edge spectrum has peaks which are transitions from 1s to convenient levels provided by 3d-4p mixing, assigned as B at 7125 eV and maximum C at 7134 eV. According to XMCD spectra, B edge has spin-down transition, however C maximum corresponds to spin-up transitions with a little peak in front due to spin-orbit coupling.
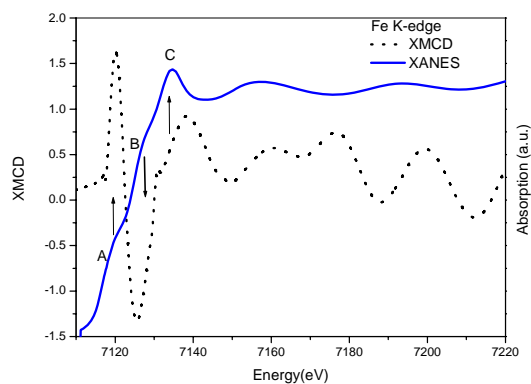
Fig. 3. Comparison of XANES and XMCD calculation of Fe K-edge absorption spectra for Fe foil. Fe K-edge absorption spectrum begin to rise at energy 7111 eV.

In contrast with metal iron, in $CuFeO_2$ structure, ferromagnetic behaviour is not observed while calculations. Iron is a ferromagnetic material; however its oxides are mostly having anti-ferromagnetic properties. In oxides, oxygen nonstoichiometry largely affects the antiferromagnetism. In delafossite $CuFeO_2$ is an example for anti-ferromagnetic oxide of Fe and triangular Fe^{+3} lattice layers are separated by nonmagnetic Cu^{+1} and O^{-2} layers [4].

Structural properties of delafossite $CuFeO_2$ were investigated by EXAFS calculation and shown in Fig. 4. Bonding process between iron (Fe) and copper (Cu), Oxygen (O) is given in the trace of photoelectrons while they are travelling out from the source (Fe) atom and back. The scattering intensities (χ) of metallic Fe with $CuFeO_2$ structure are compared as a function of wave number k. Strong and continous scattering intensity of the Fe foil structure is obvious in the figure, but weak scattering intensity of $CuFeO_2$ structure decays in a short limit. In metallic Fe foil, iron atoms are located in far distances from the others because of Coulombic forces acting on each other. The photoelectrons emitted from source iron atom in bulk Fe, travels with high kinetic energy. Large distances and weak intermedia potentials provide a long free path to the photoelectron emitted from a Fe atom with high kinetic energy. However, in $CuFeO_2$ structure, the photoelectrons lose their energy in a short limit because of the weaker oxygen (O) potentials. Oxygen atoms are located in the empty spaces between heavier Fe and Cu atoms. Occupied interatomic fields by oxygen, provide a continuous potential. Thus, emitted photoelectrons suffer extra scatterings from weak O potentials causing extra decrease in their kinetic energy and decay in a short distance.

The absorption edge and the pre-edge structure is attributed to the excitation from $2p_{3/2}$ subshells to unoccupied d levels. $3d$ levels of oxides having 5 degrees of degeneracy and bonding with neighboring O atoms cause splittings in bands with low and high energy levels. When the small atoms (O) locate closer distances to heavier atoms (Fe, Cu), wave functions of outer shell electrons of the neighboring atoms overlap. In case of resonance and if the overlapping levels have close energies, the interaction and the following overlap would be stronger. This interaction builds large hybrid molecular bands with high and low energy levels which cause changes in the electronic and magnetic properties [26]. As a matter of fact, oxygen has a key role in establishing strong structural oxides with different geometry and electronic properties [27, 28]. Beyond the pre-edge structure, a sharp peak appear at maximum of 708 eV. The higher absorption intensity of Fe L₃ edge in $CuFeO_2$ than metal Fe L₃ edge, given in figure 1, is a result of d-p hybridization between Fe $3d$- $2p$ O levels.
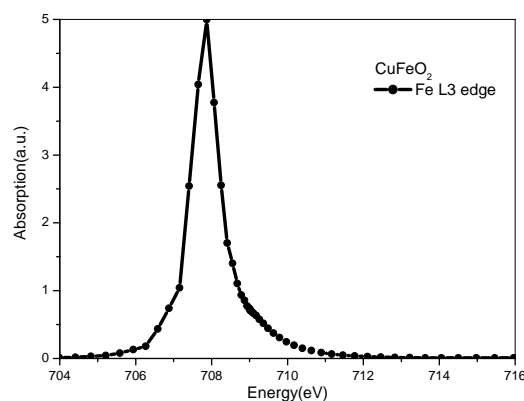
Fig. 5. Calculated XANES spectrum of Fe L₃ edge absorption in delafossite CuFeO₂ structure.

Fig. 4. EXAFS calculation comparison of scaterring intensities (χ) of Fe foil and delafossite CuFeO₂ structure in the trace of photoelectrons while they are travelling out from the source (Fe) atom and back.
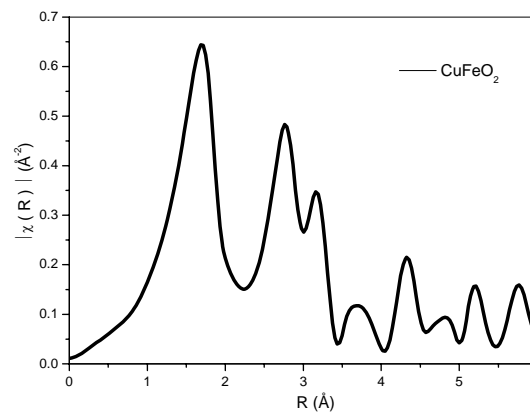
Fig. 6. Radial distribution function of delafossite CuFeO₂ crystal structure.

In Fig. 5, calculated XANES spectrum of Fe L₃ edge in $CuFeO_2$ structure is given. The absorption edge begin to rise at 705 eV and a pre-edge structure appear at 706 eV.

In Fig. 6, The Fourier transform of the scattering intensities, the radial distribution function (RDF), is given. The peaks are attributed to the nearest neighboring shells which surrounds the absorbing Fe atom in six angstroms distance. The peak distances are related with the atomic distances between the source Fe atom and the neighboring Fe, Cu or O atoms. Each peak contains information about the spherical localization of atoms in the crystal. However, informations at close distances to the source atom may superpose! In order to differentiate the information in superposed peaks and to specify certain atomic locations and types of atom one has to make fits. In Fig. 6, the first main peak contain the signals from the closest six oxygen atoms to source Fe atoms located at distance of 1.98 angstroms, however the second and the third peaks contain signals from six Fe located at 3.01angstroms and six Cu atoms at 3.34 angstroms, respectively. Table 1 shows various fitted atomic locations in $CuFeO_2$ in spherical radii of 6 angstroms.

4. Conclusions

The magnetic, electronic and crystal structure of metallic Fe foil and delafossite $CuFeO_2$ structure are investigated by XAFS and XMCD calculations. In the XMCD calculation at the Fe $L_{2,3}$ edges spin-up, spin-down transitions from 2p core to unoccupied 3d levels over the Fermi level is observed. Also due to spin orbit coupling, splitted energy levels with different electron spin orientations in Fe K-edge transitions are defined. The magnetic moment of the Fe metal is calculated as 2.27 μ_B /atom by the sum rules.

Fe is a ferromagnetic element, however in calculations of Fe containing $CuFeO_2$ structure, ferromagnetic behavior was not observed due to seperated triangular Fe^{+3} lattice layers by nonmagnetic Cu^{+1} and O^{-2} layers.

In XANES calculation of Fe L_3 core transitions in delafossite $CuFeO_2$ structure, shift in absorption energy to lower energy is observed according to hybridization of Fe 3d levels with neighboring O 2p levels.

Table 1. Atomic locations in $CuFeO_2$ structure and a Fe atom is selected as source atom.

Compound	Coordination sphere[**]	Number of atoms	Type of atom	R(A)[*]
$CuFeO_2$	Fe-O	6	O	1.982
	Fe-Fe	6	Fe	3.011
	Fe-Cu	6	Cu	3.339
	Fe-O	6	O	3.604
	Fe-Cu	6	Cu	4.496
	Fe-O	12	O	4,696
	Fe-O	6	O	5.057
	Fe-Fe	6	Fe	5.215
	Fe-Cu	12	Cu	5.411
	Fe-O	6	O	5.885
	Fe-Fe	6	Fe	5.960
	Fe-Fe	6	Fe	6.021

[*]Inter-atomic distances (±0,002Å); [**]Fe is the source atom

Crystal structure of Delafossite $CuFeO_2$ is investigated by EXAFS calculations. The atomic coordinations are defined and listed in Table 1.

References

[1] Y. Tokura, Science **312**, 1481 (2006).
[2] W. Eerenstein, N. D. Mathur, J. F. Scott, Nature **442**, 759 (2006).
[3] M. Fiebig, J. Phys. D : Appl. Phys. **38**, R123 (2005).
[4] H.Takahashi, Y. Motegi, R.Tsuchigane, M. Hasegawa, J. of Magnetism and Magnetic Materials **272-276**, 217 (2004).
[5] M. Hasegawa, M. I. Batrashevich, T. R. Zhao, H. Takei, Mater. Res. Bull. **32**, 151 (2001).
[6] O. Eriksson, B. Johansson, R. C. Albers, A. M. Boring, M. S. S. Brooks, Phys. Rev. B **42**, 2707 (1990).
[7] P. Söderlind, O. Eriksson, B. Johansson, R. C. Albers,

A. M. Boring, Phys. Rev. B **45**(12), 911 (1992).
[8] B. T. Thole, P. Carra, F. Sette, G. van der Laan, Phys. Rev. Lett. **68**, 1943 (1992).
[9] P. Carra, B. T. Thole, M. Altarelli, X. Wang, Phys. Rev. Lett. **70**, 694 (1993).
[10] J. Stöhr, H. König, Phys. Rev. Lett. **75**, 3748 (1995).
[11] R. D. Leapman, L. A. Grunes, P. L. Fejes, Phys. Rev. B **26**, 614 (1982).
[12] G. Meitzner, Microchemical J. **71**, 143 (2002).
[13] J. J. Rehr, R. C. Albers, Phys. Rev. B **41**, 8139 (1990).
[14] J. L. Erskine, E. A. Stern, Phys. Rev. B **12**, 5016 (1975).
[15] G. Schütz, W. Wagner, W. Wilhelm, P. Kienle, R. Zeller, R. Frahm, G. Materlik, Phys. Rev. Lett. **58**, 737 (1987).
[16] G. Schütz, R. Frahm, P. Mautner, R. Wienke, W. Wagner, W. Wilhelm, P. Kienle, Phys. Rev. Lett. **62**, 2620 (1989).
[17] B. D. Cullity, Introduction to Magnetic Materials,

Addison-Wesley Publishing Co., Inc., Reading, MA, 1972.

[18] F. Sette, C. T. Chen, Y. Ma, S. Modesti, N. V. Smith, in X-Ray Absorption Fine Structure, S. S. Hasnain, Ed., Ellis Horwood Limited, Chichester, England, 96, 1991.

[19] J. Stöhr, Y. Wu, B. D. Hermsmeier, M. G. Samant, G. R. Harp, S. Koranda, D. Dunham, B. P. Tonner, Science **259**, 658 (1993)

[20] L. H. Tjeng, Y. U. Idzerda, P. Rudolf, F. Sette, C. T. Chen, J. Magn. Magn. Mater. **109**, 288 (1992).

[21] J. Hunter Dunn, D. Arvanitis, N. Mårtensson, M. Tischer, F. May, M. Russo, K. Baberschke, J. Phys.: Condens. Matter. **7**, 1111 (1995).

[22] W. L. O'Brien, B. P. Tonner, Phys. Rev. B **52**, 1 (1995).

[23] A. L. Ankudinov, B. Ravel, J. J. Rehr, S. D. Conradson, Phys. Rev. B **56**, R1712 (1997).

[24] Y. Ufuktepe, G. Akgul, J. Luning, J. of Alloys and Compounds **401**, 193 (2005).

[25] J. Mustre de Leon, J. J. Rehr, S. I. Zabinsky, R. C. Albers, Phys. Rev. B **44**, 4146 (1991).

[26] G. L. Miessler, D. B. Tarr, Inorganic Chemistry, Pearson Education International, 1999.

[27] P. Serrini, V. Briois, M. C. Horillo, A. Traverse, L. Manes, Thin Solid Films **304**, 113 (1997).

[28] S. C. Tsang, R. Burch, S. Nishiyama, D. Gleeson, N. A. Cruise, A. Glidle, V. Caps, Nano-Structured Materials **12**, 999 (1999).

[*]Corresponding author: ozkendir@gmail.com